THE JOURNAL OF BIOLOGICAL CHEMISTRY VOL. 292, NO. 10, pp. 4089–4098, March 10, 2017

Localization of Protein Kinase NDR2 to Peroxisomes and Its Role in Ciliogenesis*[S]

Received for publication, January 9, 2017 Published, JBC Papers in Press, January 25, 2017, DOI 10.1074/jbc.M117.775916

Shoko Abe[‡], Tomoaki Nagai[‡], Moe Masukawa[‡], Kanji Okumoto[§], Yuta Homma[‡], Yukio Fujiki[¶], and Kensaku Mizuno[‡1]

From the [‡]Department of Biomolecular Sciences, Graduate School of Life Sciences, Tohoku University, Sendai, Miyagi 980-8578, the [§]Graduate School of Systems Life Sciences, Kyushu University, Motooka, Fukuoka 819-0395, and the [¶]Medical Institute of Bioregulation, Kyushu University, Maidashi, Fukuoka 812-8582, Japan

Edited by George M. Carman

Nuclear Dbf2-related (NDR) kinases, comprising NDR1 and NDR2, are serine/threonine kinases that play crucial roles in the control of cell proliferation, apoptosis, and morphogenesis. We recently showed that NDR2, but not NDR1, is involved in primary cilium formation; however, the mechanism underlying their functional difference in ciliogenesis is unknown. To address this issue, we examined their subcellular localization. Despite their close sequence similarity, NDR2 exhibited punctate localization in the cytoplasm, whereas NDR1 was diffusely distributed within the cell. Notably, NDR2 puncta mostly co-localized with the peroxisome marker proteins, catalase and CFP-SKL (cyan fluorescent protein carrying the C-terminal typical peroxisome-targeting signal type-1 (PTS1) sequence, Ser-Lys-Leu). NDR2 contains the PTS1-like sequence, Gly-Lys-Leu, at the C-terminal end, whereas the C-terminal end of NDR1 is Ala-Lys. An NDR2 mutant lacking the C-terminal Leu, NDR2(ΔL), exhibited almost diffuse distribution in cells. Additionally, NDR2, but neither NDR1 nor NDR2(ΔL), bound to the PTS1 receptor Pex5p. Together, these findings indicate that NDR2 localizes to the peroxisome by using the C-terminal GKL sequence. Intriguingly, topology analysis of NDR2 suggests that NDR2 is exposed to the cytosolic surface of the peroxisome. The expression of wild-type NDR2, but not NDR2(ΔL), recovered the suppressive effect of NDR2 knockdown on ciliogenesis. Furthermore, knockdown of peroxisome biogenesis factor genes (*PEX1* or *PEX3*) partially suppressed ciliogenesis. These results suggest that the peroxisomal localization of NDR2 is implicated in its function to promote primary cilium formation.

Nuclear Dbf2-related (NDR)[2] kinases are members of an NDR/large tumor suppressor (LATS) subclass of serine/threonine kinases (1, 2). NDR kinases are evolutionarily conserved from yeast to humans. Most vertebrate genomes encode two closely related NDR kinases, NDR1 and NDR2 (also known as serine/threonine kinase-38 (STK38) and STK38-like (STK38L), respectively), at distinct genomic loci. Genetic studies on NDR orthologs, such as tricornered (Trc) in the fruit fly, Sax-1 in nematodes, Cbk1p in budding yeast, and Orb6p in fission yeast, have revealed that NDR kinases play crucial roles in various cellular processes, including epidermal morphogenesis and neuronal dendritic branching and tiling in the fruit fly, neurite outgrowth in nematodes, and polarized cell growth and morphogenesis in yeast (1–4). In mammals, NDR kinases are implicated in the regulation of cell cycle progression (5), apoptosis (6), centrosome duplication (7), mitotic chromosome alignment (8), and neuronal dendrite arborization and spine development (9). In addition, *Ndr1* gene knock-out mice are predisposed to develop T-cell lymphoma (10). NDR1/2 kinases phosphorylate and negatively regulate the transcriptional co-activator, YAP1, and ablation of NDR1/2 from the intestinal epithelium promotes colon carcinogenesis (11). These results suggest that NDR1/2 have tumor-suppressive functions.

In most cases, NDR1 and NDR2 appear to share common cellular and physiological functions (5, 6, 9, 11). However, we recently showed that NDR2, but not NDR1, plays a critical role in the formation of primary cilia (12), which are antenna-like sensory organelles that sense and transmit a variety of chemical and mechanical signals from outside of the cell (13, 14). Because primary cilia are essential for the development and homeostasis of numerous tissues, defects in cilium formation cause diverse human diseases, including polycystic kidney disease, retinal degeneration, polydactyly, and brain malformation; these are commonly known as ciliopathies (13, 14). In the early stage of ciliogenesis, membrane vesicles are transported and fused to the distal end of the mother centriole to generate the "ciliary vesicle" (15). As the axoneme grows from the distal end of the mother centriole, the ciliary vesicle elongates and fuses with the plasma membrane, resulting in the extrusion of the cilium from the cell surface (15). The process of ciliary vesicle formation requires Rabin8 (a GDP-GTP exchange factor for Rab8)-mediated activation of Rab8 on the centrosome (15–17). NDR2 was

* This work was supported by Ministry of Education, Culture, Science, Sports, and Technology of Japan Grants for Scientific Research 15H04347 and 15H01197 (to K. M.) and 24247038 and 26116007 (to Y. F.). The authors declare that they have no conflicts of interest with the contents of this article.

[S] This article contains supplemental Movie S1.

[1] To whom correspondence should be addressed. Tel.: 81-22-795-6676; Fax: 81-22-795-6678; E-mail: kmizuno@biology.tohoku.ac.jp.

[2] The abbreviations used are: NDR, nuclear Dbl-related kinase; NDR1(+L), NDR1 with an additional leucine residue at the C terminus; NDR2(ΔL), NDR2 with a loss of a C-terminal leucine residue; CFP, cyan fluorescent protein; CFP-SKL, CFP with a Ser-Lys-Leu sequence at the C terminus; Pex, peroxin or peroxisome biogenesis factor; PNS, post-nuclear supernatant; PTS, peroxisomal targeting signal; ROS, reactive oxygen species; RPE, retinal pigment epithelial; ATM, ataxia telangiectasia-mutated; ANOVA, analysis of variance.

shown to be crucial for the early step of ciliogenesis by phosphorylating Rabin8 and promoting local activation of Rab8 in the vicinity of the centrosome (12). Recent studies have also identified *NDR2* (*STK38L*) as the causal gene for canine early retinal degeneration, the genetic disorder corresponding to the human ciliopathy, Leber congenital amaurosis (18, 19), which further suggests a role for NDR2 in primary cilium formation.

NDR1 and NDR2 have similar structures, sharing 87% amino acid sequence identity, and similar substrate specificities (2, 20). *In vitro* kinase assays showed that both NDR1 and NDR2 have the potential to phosphorylate Rabin8 (9, 12). However, depletion of NDR1 had no apparent effect on ciliogenesis, whereas depletion of NDR2 significantly suppressed ciliogenesis (12). Notably, the subcellular localizations of NDR1 and NDR2 differ; NDR2 exhibits vesicular localization in the cytoplasm, whereas NDR1 is distributed diffusely throughout the cytoplasm and the nucleus (12, 20). Thus, the functional difference between NDR2 and NDR1 in ciliogenesis might be due to their distinct subcellular localizations. However, the questions of which vesicles or organelles NDR2 localizes to and how NDR2, but not NDR1, localizes to vesicular particles remain unsolved. Furthermore, it is also unclear whether the vesicular localization of NDR2 is correlated to its function in ciliogenesis.

Peroxisomes are single-membrane organelles that function in numerous metabolic pathways, such as β-oxidation of very long chain and branched fatty acids, biosynthesis of ether phospholipids, and detoxification of hydrogen peroxide and reactive oxygen species (21). The biogenesis of peroxisomes is accomplished by a set of peroxisome biogenesis proteins collectively termed peroxins (Pexs) (21–25). Pex dysfunctions cause severe genetic disorders, termed peroxisome biogenesis disorders, such as Zellweger syndrome (21–25). The majority of peroxisomal matrix proteins contain a peroxisomal targeting signal type 1 (PTS1) motif, consisting of the tripeptide SKL or its conserved variants, at their C-terminal end (26–28). PTS1-containing proteins are recognized by the PTS1 receptor Pex5p in the cytoplasm and are imported to the peroxisomes via the docking and translocation machinery on the peroxisomal membranes (21–25).

In this study, we found that NDR2, but not NDR1, localizes to the peroxisome. We provide evidence that the C-terminal GKL sequence of NDR2 functions as the peroxisomal targeting signal. Furthermore, the expression of wild-type NDR2, but not its peroxisome-non-targeting mutant, rescued the inhibitory effect of NDR2 knockdown on ciliogenesis. Knockdown of the *PEX* gene (*PEX1* or *PEX3*) partially suppressed ciliogenesis. Collectively, our results suggest that the peroxisomal localization of NDR2 is crucial for its function to promote primary cilium formation.

Results

NDR2 Localizes to the Peroxisomes—Previous studies have shown that NDR2 exhibits a punctate localization in the cytoplasm, whereas NDR1 is distributed diffusely in both the cytoplasm and the nucleus (12, 20). To define the subcellular localization of NDR2, human telomerase-immortalized retinal pigment epithelial-1 (RPE1) cells were transfected with the plasmid encoding N-terminally yellow fluorescent protein (YFP)-tagged NDR2 and immunostained with specific antibodies against several organelle marker proteins. Comparison of the punctate localization of YFP-NDR2 with the localization of organelle marker proteins revealed that YFP-NDR2 co-localized well with catalase (a marker for peroxisomes) but not with early endosome antigen 1 (EEA1, a marker for early endosomes), *cis*-Golgi matrix protein of 130 kDa (GM130, a marker for *cis*-Golgi networks), microtubule-associated protein 1 light chain 3 (LC3, a marker for autophagosomes), or lysosome-associated membrane protein-1 (LAMP1, a marker for lysosomes) (Fig. 1). These results suggest that NDR2 localizes to the peroxisome.

To further examine the localization of NDR2, we compared the localization of YFP-NDR2 with that of CFP-SKL (cyan fluorescent protein carrying a typical PTS1 sequence, Ser-Lys-Leu, at its C terminus). YFP-NDR2 mostly co-localized with CFP-SKL (Fig. 2). In contrast, control YFP and YFP-NDR1 distributed diffusely in the cell (Fig. 2). Time lapse fluorescence analysis of RPE1 cells co-expressing YFP-NDR2 and CFP-SKL further demonstrated that these proteins co-localized well during the observation period (supplemental Movie S1). These results indicate that NDR2 localizes to the peroxisome.

Subcellular Fractionation Analysis—The intracellular localization of NDR2 was further examined by subcellular fractionation analysis. When the post-nuclear supernatant (PNS) fraction of YFP-NDR2-expressing HeLa cells was fractionated into the organellar and cytosolic fractions, YFP-NDR2 was detected in both fractions (Fig. 3*A*). Upon further fractionation of the PNS fraction by iodixanol density gradient ultracentrifugation, YFP-NDR2 was detected and co-sedimented well with a peroxisomal protein, Pex14p (Fig. 3*B*, *lanes 8* and *9*), which further supports the peroxisomal localization of NDR2. To examine the localization of endogenous NDR2, the PNS fraction of RPE1 cells was separated to the organellar and cytosolic fractions and analyzed by immunoblotting with an anti-NDR2 antibody. NDR2 was detected in both fractions, although less in the organellar fraction (Fig. 3*C*), which suggests that endogenous NDR2, at least in part, is localized at the organelles. Further fractionation or immunostaining analysis using an anti-NDR2 antibody failed to detect endogenous NDR2, probably because the expression level of endogenous NDR2 is below the detection limit of the antibody.

The C-terminal GKL Motif Is Required for the Peroxisomal Localization of NDR2—The amino acid sequences of NDR1 and NDR2 are highly homologous. The overall identity of human or mouse NDR1 and NDR2 is 87%, and the identity of their protein kinase domains is 91% (1, 20). However, there is a noticeable difference in the C-terminal sequences of these proteins: NDR2 has the C-terminal sequence YMKAGKL, whereas NDR1 has YMKAAK (Fig. 4*A*). The difference in the C-terminal sequences of NDR1 and NDR2 is conserved in mammals. The C-terminal GKL sequence of NDR2 is closely related to the PTS1 consensus sequence (S/A/C)(K/R/H)(L/M) (26–28), which prompted us to examine the possibility that NDR2 is localized to the peroxisome through the C-terminal GKL motif and that NDR1 is not localized to the peroxisome due to the absence of the C-terminal leucine residue. To explore this possibility, we constructed expression plasmids encoding a YFP-

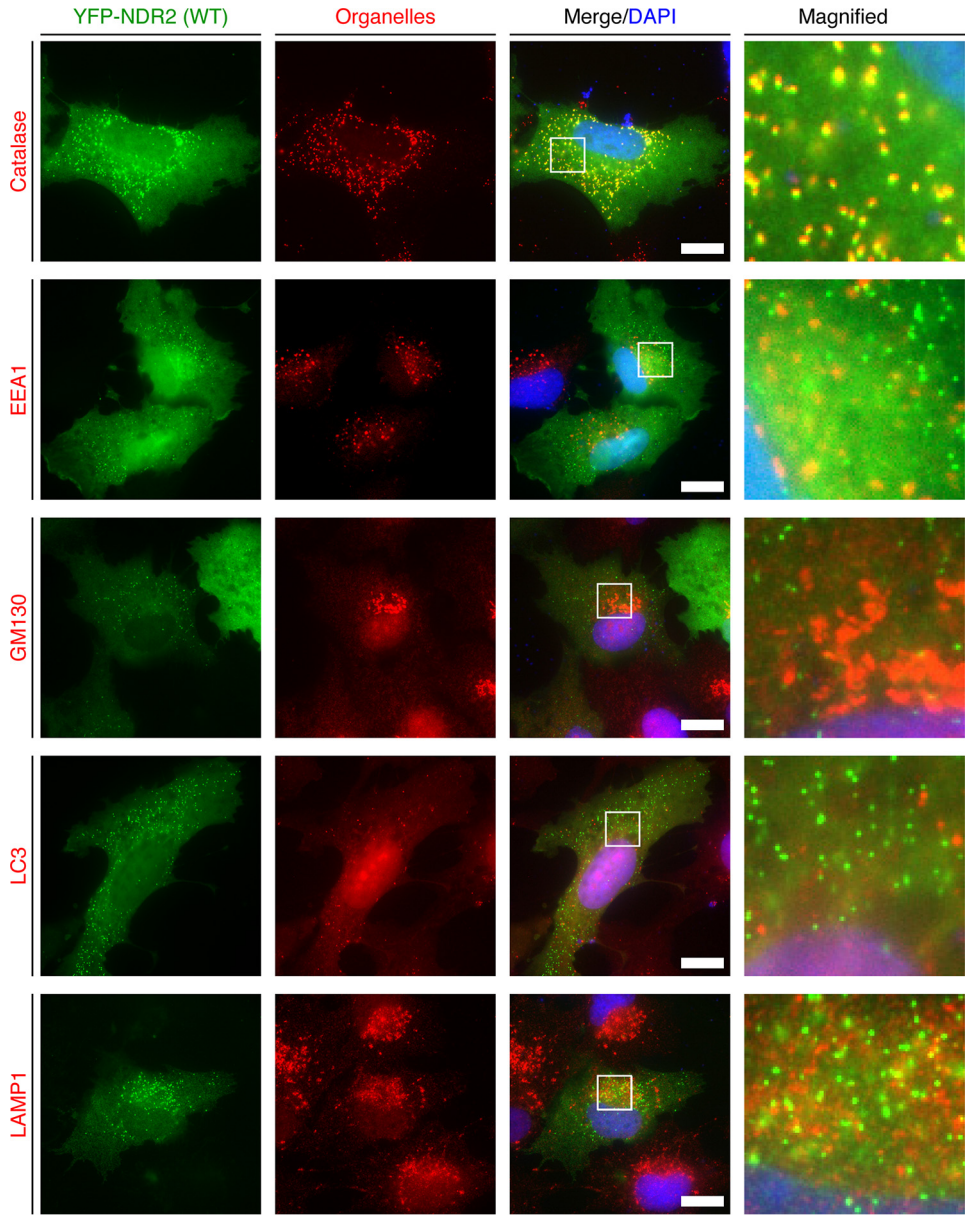

FIGURE 1. **NDR2 co-localizes with catalase.** RPE1 cells were transfected with the plasmid for YFP-NDR2 and cultured for 24 h. Cells were fixed and then imaged by YFP fluorescence (*green*) and stained with the antibodies against catalase, EEA1, GM130, LC3, and LAMP1, as indicated (*red*). DNA was stained with DAPI (*blue*). Merged fluorescence images are shown in the *third column*. *Magnified images* of the *white boxes* in the *third column* are shown in the *fourth column*. *Scale bar*, 20 μm.

tagged NDR2 mutant with a deletion of the C-terminal leucine, YFP-NDR2(ΔL), and a YFP-tagged NDR1 mutant carrying an additional leucine at the C-terminal end, YFP-NDR1(+L) (Fig. 4*A*), and examined their peroxisomal localization by co-expressing them with CFP-SKL. The expression of each protein was confirmed by immunoblot analysis with an anti-GFP antibody (Fig. 4*B*). YFP-NDR2(WT) showed a punctate co-localization with CFP-SKL (Fig. 2*A*), but YFP-NDR2(ΔL) distributed diffusely in the cytoplasm and the nucleus (Fig. 4*C*). Conversely, YFP-NDR1(WT) distributed diffusely in the cytoplasm and the nucleus (Fig. 2*A*), but YFP-NDR1(+L) exhibited a punctate localization in the cytoplasm and co-localized with CFP-SKL (Fig. 4*C*). Quantitative analysis showed that the deletion of the C-terminal leucine significantly decreased the number of cells with punctate localization of NDR2, and the addition of leucine at the C terminus significantly increased the number of cells with punctate localization of NDR1 (Fig. 4*D*). These results indicate that the leucine residue in the C-terminal GKL motif of NDR2 is required for its localization to the peroxisome and that the distinct localization between NDR2 and NDR1 is primarily due to the difference between their C-terminal sequences.

NDR2, but Not NDR1, Binds to Pex5p—The PTS1 signal of peroxisomal proteins is recognized by a receptor protein, Pex5p, which binds to the PTS1 sequence and translocates cargo proteins to the peroxisome through its interaction with a docking complex (21–25). There are two splicing variants of Pex5p: a short form (Pex5pS) and a long form (Pex5pL), of which Pex5pS is exclusively involved in PTS1-containing protein import to the peroxisome (23, 29). To examine whether NDR2 is localized to the peroxisome through its binding to

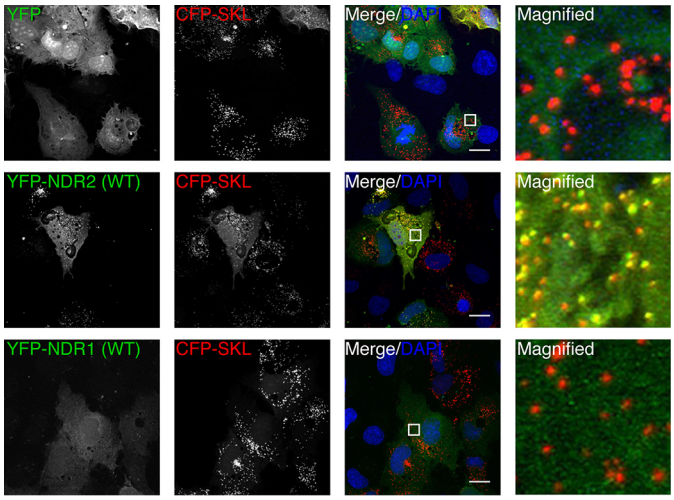

FIGURE 2. **NDR2, but not NDR1, co-localizes with CFP-SKL.** RPE1 cells were co-transfected with the plasmid for CFP-SKL and the plasmids for YFP, YFP-NDR2, or YFP-NDR1 and cultured for 24 h. Cells were fixed and imaged by YFP (*green*) and CFP (*red*) fluorescence. DNA was stained with DAPI (*blue*). Merged fluorescence images are shown in the *third column*. *Magnified images* of the *white boxes* in the *third column* are shown in the *fourth column*. *Scale bar*, 20 μm.

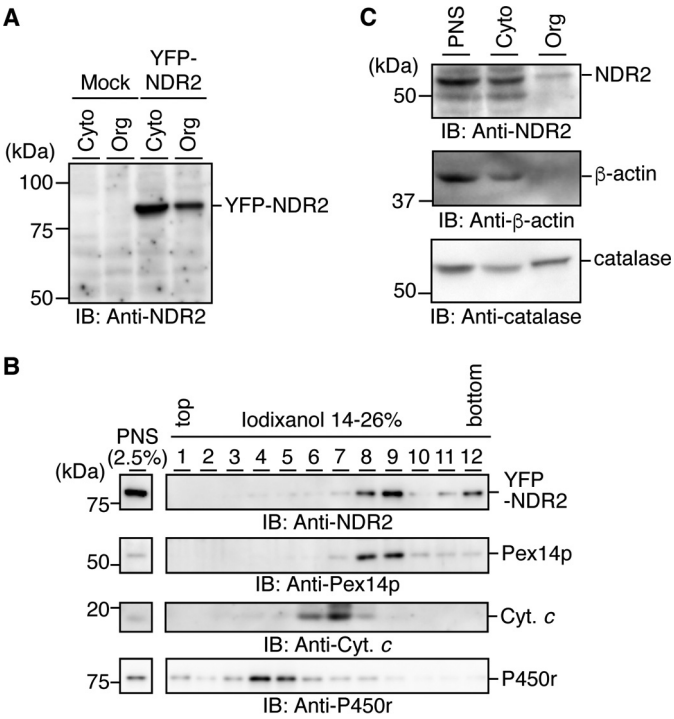

FIGURE 3. **Subcellular fractionation analysis of NDR2.** *A*, subcellular fractionation of YFP-NDR2. PNS fractions of HeLa cells (*Mock*) or YFP-NDR2-expressing HeLa cells were separated into the cytosolic (*Cyto*) and organellar (*Org*) fractions. Equal aliquots of each fraction were analyzed by immunoblotting (*IB*) with an anti-NDR2 antibody. *B*, localization of YFP-NDR2 in the peroxisomal fraction. PNS fractions of YFP-NDR2-expressing HeLa cells were separated by ultracentrifugation on a 14–26% iodixanol density gradient. The gradient was collected into 12 fractions. Equal aliquots of each fraction and PNS fraction (2.5% of the loaded amount) were analyzed by immunoblotting with antibodies against NDR2, Pex14p, cytochrome *c* (*Cyt. c*), and P450 reductase (*P450r*). *C*, subcellular fractionation of endogenous NDR2. PNS fractions of RPE1 cells were separated into cytosolic and organellar fractions. Equal aliquots of each fraction were analyzed by immunoblotting with antibodies against NDR2, β-actin, and catalase.

Pex5pS, we analyzed the binding ability of NDR2 with Pex5pS using co-immunoprecipitation assays. The construct YFP-NDR2 or -NDR2(ΔL) was co-expressed with FLAG-tagged Pex5pS in 293T cells and immunoprecipitated with an anti-GFP antibody, and the precipitates were analyzed by immunoblotting with an anti-FLAG antibody. FLAG-Pex5pS was co-precipitated with NDR2(WT) but not with NDR2(ΔL) (Fig. 5), which suggests that NDR2 is localized to the peroxisome by the association with Pex5pS and that the C-terminal GKL motif is required for NDR2 binding to Pex5pS. Additionally, FLAG-Pex5pS was co-precipitated with NDR1(+L), but not with NDR1(WT) (Fig. 5), which suggests that the C-terminal AKL motif of NDR1(+L) is recognized by Pex5pS for localization to the peroxisome.

NDR2 Is Exposed to the Cytosol—To examine whether NDR2 is imported into the peroxisomal matrix or resides on the outside of the peroxisomal membrane, YFP-NDR2 was expressed in RPE1 cells, and the PNS fraction of the cells was subjected to a proteinase K sensitivity assay. YFP-NDR2 was detected in the mock-treated PNS fraction (Fig. 6*A*, *lane 1*) but was not detectable after proteinase K treatment (Fig. 6*A*, *lane 2*). Under similar conditions, a peroxisomal membrane protein PMP70 was sensitive to proteinase K treatment, whereas catalase, a peroxisomal matrix protein control, was mostly protected against the protease treatment (Fig. 6, *B* and *C*, *lane 2*). All of these proteins were degraded by the protease treatment in the presence of Triton X-100 (Fig. 6, *A*–*C*, *lane 3*). These results suggest that NDR2 is not a peroxisomal matrix protein and that at least a part of the molecule resides on the cytosolic side of the peroxisomal membrane.

The C-terminal GKL Motif Is Required for the Function of NDR2 to Promote Ciliogenesis—We showed previously that the knockdown of NDR2 significantly suppressed primary cilium formation but that knockdown of NDR1 had no overt effect on ciliogenesis, indicating that NDR2, but not NDR1, plays a critical role in ciliogenesis (12). To explore the role of the peroxisomal localization of NDR2 for its function in ciliogenesis, we examined whether the expression of siRNA-resistant mouse NDR2 (WT or ΔL) could ameliorate the inhibitory effect of NDR2 knockdown on ciliogenesis. RPE1 cells were treated with control or *NDR2*-targeting small interfering RNA (siRNA) and cultured for 24 h and then serum-starved for 48 h. Then the number of ciliated cells was counted by staining acetylated (Ac)-tubulin. As reported (12), cell treatment with *NDR2* siRNA reduced the levels of NDR2 protein (Fig. 7*A*) and significantly suppressed ciliogenesis, compared with control siRNA treatment (Fig. 7, *B* and *C*). Expression of YFP-tagged, siRNA-resistant NDR2(WT) significantly rescued primary cilium formation in NDR2-depleted cells, but expression of YFP-NDR2(ΔL) did not (Fig. 7, *B* and *C*), indicating that the C-terminal leucine residue is required for the function of NDR2 in ciliogenesis and that the peroxisomal localization of NDR2 is correlated to its function in ciliogenesis. The expression of YFP-NDR1 did not rescue ciliogenesis in NDR2-depleted cells (Fig. 7, *B* and *C*). Notably, the expression of YFP-NDR1(+L) slightly, but not significantly, restored ciliogenesis in NDR2-depleted cells (Fig. 7, *B* and *C*). These results suggest that per-

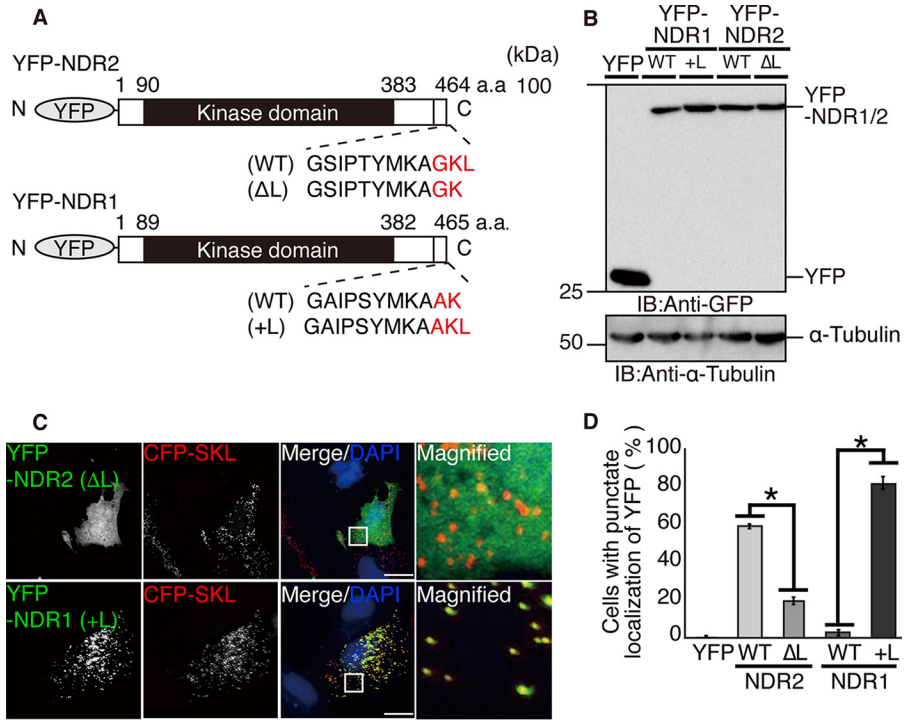

FIGURE 4. **The C-terminal GKL motif is required for the peroxisomal localization of NDR2.** *A*, schematic structures of YFP-tagged mouse NDR2, NDR1, and their mutants used in this study. The C-terminal amino acid sequences of NDR2, NDR1, and their mutants are indicated. *B*, immunoblot analysis of the expression of YFP, YFP-NDR2, YFP-NDR1, and their mutants. RPE1 cells were transfected with the plasmids each encoding YFP, YFP-NDR2, YFP-NDR1, or their mutants and cultured for 24 h, and cell lysates were analyzed by immunoblotting (*IB*) with anti-GFP and anti-α-tubulin antibodies (as a loading control). *C*, subcellular localization of NDR2(ΔL) and NDR1(+L). RPE1 cells were co-transfected with the plasmids encoding CFP-SKL and YFP-NDR2(ΔL) or YFP-NDR1(+L) and analyzed by YFP (*green*) and CFP (*red*) fluorescence. DNA was stained with DAPI (*blue*). Merged fluorescence images are shown in the *third column*. *Magnified images* of the *white boxes* in the *third column* are shown in the *fourth column*. *Scale bar*, 20 μm. *D*, quantitative analysis of the percentage of cells in which YFP fluorescence exhibits punctate co-localization with CFP-SKL. Data are expressed as the means ± S.E. (*error bars*) of three independent experiments (>100 cells/experiment, one-way ANOVA followed by Dunnett's test). *, $p < 0.01$.

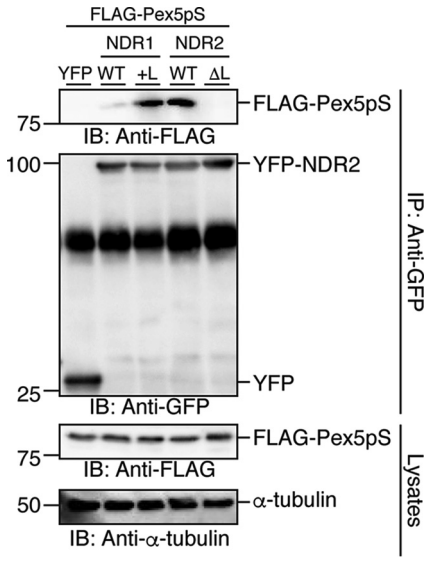

FIGURE 5. **NDR2 and NDR1(+L), but neither NDR2(ΔL) nor NDR1, bind to Pex5p.** HEK293T cells were co-transfected with the plasmids encoding FLAG-tagged Pex5pS and YFP-tagged NDR2, NDR1, or their mutants. Cell lysates were subjected to immunoprecipitation (*IP*) with an anti-GFP antibody and analyzed by immunoblotting (*IB*) with anti-FLAG and anti-GFP antibodies.

oxisomal localization alone is not sufficient for NDR1(+L) to replace the function of NDR2 in ciliogenesis.

Knockdown of PEX1 or PEX3 Suppresses Ciliogenesis—As the peroxisomal localization of NDR2 is correlated to its function in ciliogenesis, we next examined whether the knockdown of *PEX1* or *PEX3* (genes essential for peroxisome biogenesis) affects ciliogenesis. RPE1 cells were transfected with siRNAs targeting *PEX1* or *PEX3*, cultured for 24 h, and then cultured for 48 h under serum-starved conditions. Two independent siRNAs against *PEX1* and *PEX3* effectively decreased the expression of the respective transcripts in RPE1 cells (Fig. 8*A*). Treatment with *PEX1* or *PEX3* siRNAs considerably reduced the frequency of ciliated cells, as compared with control siRNA treatment (Fig. 8*B*). More severe suppression of ciliogenesis was observed by knockdown of Tau tubulin kinase-2 (*TTBK2*), an essential gene for ciliogenesis (30–32). These data suggest that the peroxisome plays a role in primary cilium formation.

Effect of NDR2 Knockdown on Peroxisome Assembly—The peroxisomal localization of NDR2 raises the possibility that it might be involved in peroxisome formation. To examine this possibility, we analyzed the effect of NDR2 knockdown on the formation of peroxisomes. RPE1 cells were transfected with control siRNA or *NDR2*-targeting siRNAs, and the formation of peroxisomes was analyzed by immunostaining using an anti-catalase antibody. Treatment with *NDR2*-targeting siRNAs had no apparent effect on the punctate localization of catalase (Fig. 9), which suggests that NDR2 does not play an essential role in peroxisome formation.

Discussion

Despite high sequence similarity, NDR1 and NDR2 display distinct subcellular localizations; NDR2 localizes to the vesicu-

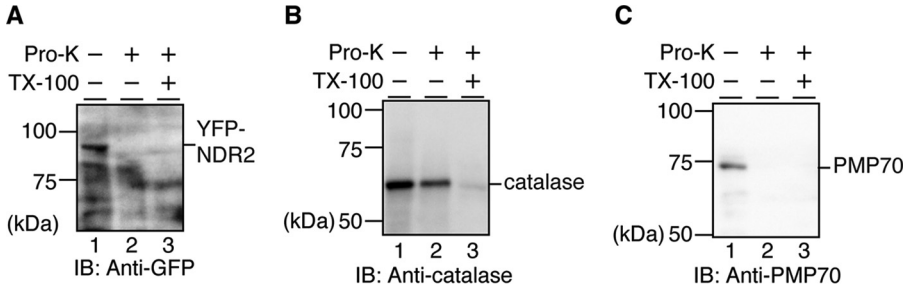

FIGURE 6. **Topology analysis of NDR2.** RPE1 cells were transfected with the plasmid for YFP-NDR2, and the PNS fraction was prepared. The PNS fraction was mock-treated (−) or treated with proteinase K (*Pro-K*) (+) in the absence (−) or presence (+) of Triton X-100 (*TX-100*). The reaction mixture was ultracentrifuged, and the resulting pellets were analyzed by SDS-PAGE and immunoblotting (*IB*) with antibodies against GFP (*A*), catalase (*B*), and PMP70 (*C*).

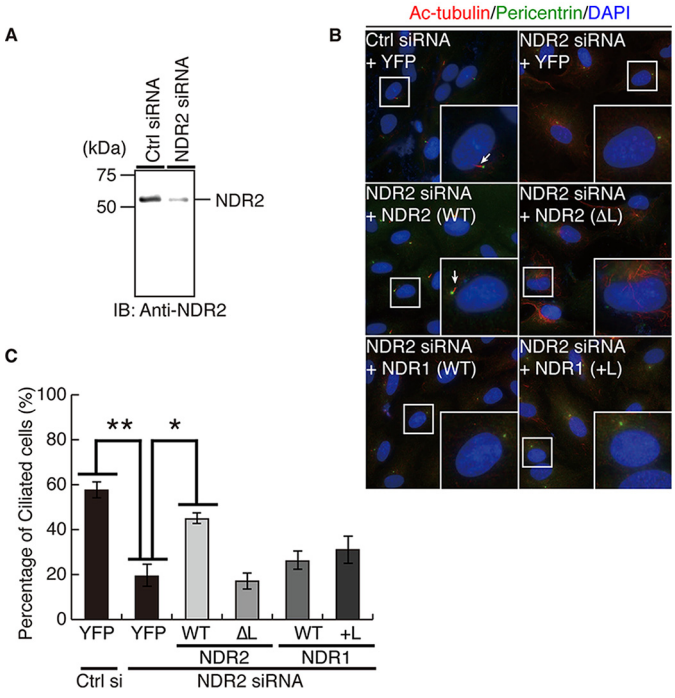

FIGURE 7. **The C-terminal GKL motif is required for NDR2 to promote ciliogenesis.** *A*, effect of *NDR2*-targeting siRNA on the expression of endogenous NDR2. RPE1 cells were transfected with human *NDR2*-targeting siRNA and cultured for 72 h, and lysates were analyzed by immunoblotting (*IB*) with an anti-NDR2 antibody. *B*, effects of expression of YFP, YFP-NDR2 (WT or ΔL), or YFP-NDR1 (WT or +L) on the ciliogenesis of NDR2 knockdown cells. RPE1 cells were transfected with the plasmids coding for YFP or YFP-tagged mouse NDR2, NDR1, or their mutants and cultured for 4 h. Then cells were transfected with human *NDR2*-targeting siRNA, cultured for 24 h, and serum-starved for 48 h. Cells were fixed and stained with anti-Ac-tubulin (*red*) and anti-pericentrin (*green*) antibodies. DNA was stained with DAPI (*blue*). *Insets*, *magnified images* (× 2.7) of the *white boxes*. *Arrows*, primary cilia. *C*, quantitative analysis of the percentage of ciliated cells. RPE1 cells were treated as in *B*. Data are expressed as the means ± S.E. (*error bars*) of three independent experiments (>100 cells/experiment, one-way ANOVA followed by a Dunnett's test). *, $p < 0.05$; **, $p < 0.01$.

lar compartments in the cytoplasm, whereas NDR1 is diffusely distributed within cells. In this study, we found that NDR2 co-localizes with catalase and CFP-SKL, indicating that NDR2 localizes to the peroxisomes. Deletion of the single leucine residue from the C-terminal GKL sequence abrogated the abilities of NDR2 to bind to the PTS1 receptor Pex5pS and to localize to the peroxisome. These observations suggest that NDR2 localizes to the peroxisome by using the C-terminal GKL motif as the peroxisomal targeting signal. Previous mutation analyses revealed that mutant proteins harboring the C-terminal GKL motif are capable of localizing to the peroxisome, albeit at a lower efficiency than those containing the conventional SKL motif (33, 34), which supports our finding that the C-terminal GKL motif of NDR2 acts as the peroxisomal targeting signal. To our knowledge, NDR2 is the first known endogenous protein that localizes to the peroxisome by utilizing the GKL sequence as the peroxisomal targeting signal in mammalian cells.

In contrast to NDR2, NDR1 contains a C-terminal AK sequence, which does not conform to the consensus sequence of PTS1. We showed that NDR1 is diffusely distributed in cells, but its mutant NDR1(+L), containing an additional leucine at the C-terminal end, localizes to the peroxisome. NDR1(+L), but not wild-type NDR1, bound to Pex5pS. These results suggest that NDR1(+L) localizes to the peroxisome by using the artificially constructed C-terminal AKL sequence as the peroxisomal targeting signal. Thus, the distinct localization of NDR2 and NDR1 is due to the presence or absence of the single leucine residue at the C-terminal end of each protein, respectively.

We previously showed that knockdown of NDR2, but not NDR1, suppressed primary cilium formation in RPE1 cells (12), indicating that NDR2, but not NDR1, plays a crucial role in primary cilium formation. In this study, we showed that the expression of an siRNA-resistant wild-type NDR2, but not NDR2(ΔL), significantly ameliorated the suppressive effect of NDR2 knockdown on ciliogenesis. Furthermore, knockdown of *PEX1* or *PEX3* partially suppressed ciliogenesis. These results suggest that the peroxisomal localization of NDR2 is critical for its function to promote ciliogenesis. Expression of NDR1 also failed to restore the NDR2 knockdown-induced suppression of ciliogenesis. Notably, expression of the peroxisome-targeting NDR1(+L) also did not significantly counter the NDR2 knockdown-induced suppression of ciliogenesis. This result suggests that peroxisomal localization alone is not sufficient for NDR1 to promote ciliogenesis and that a yet uncharacterized difference in the properties of NDR1 and NDR2, such as target specificity, efficiency of enzyme activity, or regulation mechanism of enzyme activity, might also contribute to their functional disparity in promoting ciliogenesis.

Rabin8 and its downstream target Rab8 play crucial roles in ciliary vesicle formation in the early steps of ciliogenesis (15–17). NDR2 was shown to promote ciliogenesis via Rabin8 phosphorylation, which leads to local activation of Rab8 at the centrosome (12). It is unclear why the peroxisomal localization of NDR2 is favorable for its function in cilium formation. Because time-lapse fluorescence analysis of serum-starved RPE1 cells

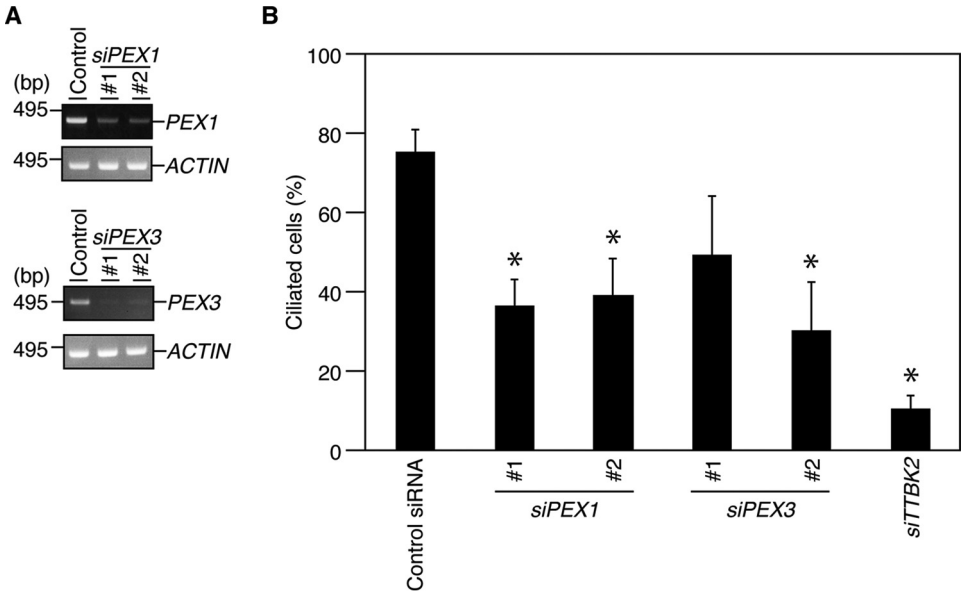

FIGURE 8. **Knockdown of *PEX1* or *PEX3* suppresses ciliogenesis.** *A*, knockdown efficiency of *PEX1*- or *PEX3*-targeting siRNAs, as measured by RT-PCR. RPE1 cells were transfected with control siRNA or *PEX1*- or *PEX3*-targeting siRNAs and cultured for 72 h, and total RNAs were subjected to RT-PCR analysis. *B*, effects of *PEX1* or *PEX3* knockdown on ciliogenesis. RPE1 cells were transfected with control siRNA or siRNAs targeting *PEX1*, *PEX3*, or *TTBK2*, cultured for 24 h, and then serum-starved for 48 h. The percentages of ciliated cells were counted as in Fig. 7*C*. Data are expressed as the means ± S.E. (*error bars*) of three independent experiments (>100 cells/experiment, one-way ANOVA followed by Dunnett's test). *, $p < 0.05$, compared with control siRNA-transfected cells.

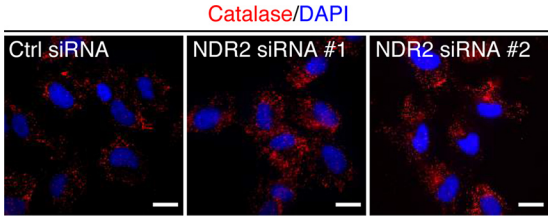

FIGURE 9. **Knockdown of NDR2 has no apparent effect on peroxisome formation.** RPE1 cells were treated with 10 nM control or *NDR2*-targeting siRNAs and cultured for 48 h. Cells were fixed and stained with an anti-catalase antibody (*red*). DNA was stained with DAPI (*blue*). *Scale bar*, 20 μm.

revealed that NDR2-carrying vesicles (identified herein as peroxisomes) are frequently associated with the centrosome (12) and that Rabin8 accumulates to the centrosome upon serum starvation (12, 15–17), the peroxisomal localization of NDR2 might be helpful to mediate the effective phosphorylation of Rabin8 at the centrosome after serum starvation. We showed that NDR2 is sensitive to proteinase K treatment, suggesting that at least a part of NDR2 is exposed to the cytosol. Thus, it is likely that NDR2 on the cytosolic side of the peroxisome is accessible to Rabin8 accumulating on the centrosome.

Peroxisomes are generally known to function to regulate the metabolism of lipids and reactive oxygen species (21), but recent studies have demonstrated a novel function of peroxisomes as signaling platforms (35–40). For example, the peroxisome functions as the platform for the signaling of reactive oxygen species (ROS)-induced activation of tuberous sclerosis complex 1/2 (TSC1/2) (which is a GTPase-activating protein for Rheb GTPase) and the subsequent inhibition of Rheb and mammalian target of rapamycin complex 1 (mTORC1) (36). The signaling components, TSC1/2, Rheb, and mTORC1, are localized on the cytosolic surface of the peroxisomal membrane. TSC2 binds to the peroxisomal matrix protein receptor Pex5p through the internal PTS1-like sequence motif, but it resides on the outside of the peroxisomal membrane. TSC2 mutants lacking the ability to bind Pex5p are ineffective for ROS-induced mTORC1 inhibition, indicating that the Pex5p-mediated peroxisomal membrane localization of TSC2 is critical for this response (36). A protein kinase, ataxia telangiectasia-mutated (ATM), also binds to Pex5p and is localized to the outer surface of the peroxisome (37, 38). ROS stimulate the kinase activity of peroxisomal ATM, which induces mTORC1 inhibition and ULK1 activation via TSC1/2 activation, as well as the phosphorylation and ubiquitination of Pex5p, resulting in the ROS-induced autophagy of peroxisomes (pexophagy) (38). Peroxisomes also function as the signaling platform for antiviral innate immunity responses (39, 40). Mitochondrial antiviral signaling protein (MAVS) is an organelle-bound adaptor protein for RIG-I-like receptors, which detect the double stranded RNAs of RNA viruses in the cytoplasm (39, 40). MAVS localizes on both peroxisomes and mitochondria. Upon viral infection, peroxisomal MAVS triggers the immediate expression of antiviral factors that provide a transient antiviral response; this response is independent of mitochondrial MAVS (39, 40). Together, these results suggest that the peroxisome serves not simply as a metabolic organelle but also as a signaling platform. The localization of NDR2 at the peroxisome suggests the possible role of this organelle as the platform for NDR2-mediated reactions as well.

Similar to TSC2 and ATM, NDR2 binds to Pex5p through the PTS1-like sequence motif and appears to reside on the exterior of the peroxisomal membrane. This is in contrast to most PTS1-harboring proteins, which are imported into the matrix of the peroxisome (21–25). How NDR2 is localized to the outside of the peroxisomal membrane remains intriguing. Because Pex5p associated with peroxisomes partly behaves as an integral membrane protein (41, 42), it is conceivable that such Pex5p recruits and tethers NDR2 to the cytosolic side of the

peroxisome. It is also possible that NDR2 is recruited to the peroxisome by Pex5p and then tethered to the membrane by any unknown NDR2-anchoring factor(s). Further studies are required to address this point.

Knockdown of NDR2 had no apparent effect on peroxisome assembly, suggesting that NDR2 has no or little contribution to the process of peroxisome biogenesis, at least under our experimental conditions. However, the possibility that NDR2 has the function to regulate peroxisome biogenesis under distinct conditions and/or peroxisomal metabolic functions by modifying peroxisomal enzymes cannot be excluded. Although databases such as PhosphoSite indicate that many Pex proteins and peroxisomal enzymes are phosphorylated, little is known about the physiological roles of phosphorylation of these proteins in the biogenesis and functions of peroxisomes. The roles of NDR2 in peroxisome biogenesis and function deserve further investigation.

The present study demonstrates the hitherto unrealized involvement of peroxisomes in primary cilium formation, which might open up a new line of investigation toward understanding the novel pathophysiological role of the peroxisome. Very recently, Pex6p was shown to localize to the connecting cilia of retinal photoreceptor cells, and homozygous mutation of the *PEX6* gene was found to cause retinal degeneration, deafness, and microcephaly (43). These symptoms considerably overlap with those associated with ciliopathy and centriole dysfunction (13, 14, 44). Further studies on the possible linkage of peroxisome biogenesis to cilium and centriole formation will pave the way to a better understanding of the mechanisms underlying peroxisome biogenesis disorders, ciliopathies, and their relationships.

Experimental Procedures

Antibodies—The antibodies used in this study were purchased as follows: rabbit polyclonal antibodies against EEA1 (MBL (Nagoya, Japan), PM062), GM130 (MBL, PM061), and GFP (Invitrogen, A6455), pericentrin (BioLegend (San Diego, CA) Poly19237), Alexa Fluor 633-labeled anti-rabbit IgG (Invitrogen, A21069), Alexa Fluor 633-labeled anti-mouse IgG (Invitrogen, A21052), and Alexa Fluor 568-labeled anti-mouse IgG (Invitrogen, A11031) and monoclonal antibodies against catalase (AbFrontier (Seoul, Korea), 1A1; Sigma-Aldrich, CAT-505), LC3 (MBL, 4E12), LAMP1 (Santa Cruz Biotechnology, Inc. (Dallas, TX), H4A3), cytochrome *c* (BD Biosciences, 556433), P450 reductase (Santa Cruz Biotechnology, sc-25270), PMP70 (Sigma-Aldrich, 70-18), FLAG (Sigma-Aldrich, M2), and Ac-tubulin (Sigma-Aldrich, 6-11-B). Rabbit polyclonal antibodies against rat Pex14p were as described (45). Rabbit polyclonal antibodies against NDR2 were raised against the peptide (amino acid residues 417–433) in the C-terminal region of NDR2, as described previously (12).

Plasmid Construction—The cDNAs encoding mouse NDR1 and NDR2 were PCR-amplified from a mouse cDNA library. To construct the cDNA plasmids coding for YFP-tagged NDR1 and NDR2, the PCR-amplified cDNAs were subcloned into pEYFP-C1 (Clontech, Mountain View, CA). The cDNA plasmids coding for NDR1(+L) and NDR2(ΔL) were constructed using the QuikChange site-directed mutagenesis kit (Stratagene, Santa Clara, CA). The cDNA plasmid for CFP-SKL was constructed by inserting the SKL-coding sequence at the 3′ terminus into the multiple cloning site of pECFP-C1 (Clontech). The cDNA plasmid coding for FLAG-tagged Pex5pS (FLAG-His_6-Pex5pS/pcDNA3.1 Zeo) was constructed as described previously (46). The Stealth small interfering RNAs (siRNAs) were purchased from Invitrogen. The siRNA targeting sequences were as follows: siNDR2#1 (5′-CAG AAU UGG AAA UAG UGG AGU AGA A-3′), siNDR2#2 (5′-GGC CAG CAG CAA UCC CUA UAG AAA U-3′), siPEX1#1 (5′-CCA AAG CAA UCU GUA AAG AAG CAU U-3′), siPEX1#2 (5′-UCC UCC UGA UCA GGU GUC ACG UCU U-3′), siPEX3#1 (5′-GGG AGG AUC UGA AGA UAA UAA GUU U-3′), siPEX3#2 (5′-UAU UUA CCU GGA UAA UGC AGC AGU U-3′), and siTTBK2 (5′-UGG CUU GGC UCG ACA AUU U-3′).

Cell Culture and Transfection—Human immortalized RPE1 cells were a gift from H. Nakanishi (Kumamoto University, Kumamoto, Japan) and were cultured in Dulbecco's modified Eagle's medium/F-12 (Wako Pure Chemical Industries, Osaka, Japan) supplemented with 10% fetal calf serum. Human embryonic kidney HEK293T cells were purchased from the American Type Culture Collection (ATCC (Manassas, VA), CRL-3216) and cultured in Dulbecco's modified Eagle's medium supplemented with 10% fetal calf serum. Plasmids were transfected into cells using the FuGENE-HD or FuGENE-6 transfection reagent (Promega, Tokyo, Japan) following the manufacturer's instructions.

Immunofluorescence Staining—RPE1 cells were grown on coverslips in 35-mm dishes. Cells were fixed with 10% trichloroacetic acid for 15 min or 4% paraformaldehyde at 37 °C for 15 min, followed by permeabilization with 0.1% Triton X-100 for 5 min. Cells were then incubated overnight at 4 °C with appropriate primary antibodies that were diluted with 2% fetal calf serum. Alexa Fluor 633-labeled anti-mouse IgG or anti-rabbit IgG antibodies were used as secondary antibodies. DNA was stained with 4′,6-diamidino-2-phenylindole (DAPI). Fluorescent images were obtained using an inverted fluorescence microscope (Leica (Wetslar, Germany), DMI6000B) equipped with a Plan-Apochromat ×63 oil immersion objective lens (numeric aperture 1.3) and processed using ImageJ software (National Institutes of Health, Bethesda, MD).

Co-immunoprecipitation Assay—293T cells were co-transfected with FLAG-His_6-Pex5pS and YFP-tagged NDR1/2 and cultured for 24 h. Cells were lysed in lysis buffer (50 mM Tris-HCl, pH 7.5, 1% Triton X-100, 10% glycerol, 150 mM NaCl, 50 mM NaF, 1 mM Na_3VO_4, 10 μg/ml leupeptin, and 1 mM dithiothreitol (DTT)) and centrifuged at 15,000 rpm for 10 min. The supernatants were precleared by incubation with nProtein A-Sepharose 4 Fast Flow (GE Healthcare, Little Chalfont, UK) for 1 h at 4 °C and then centrifuged at 15,000 rpm for 10 min. The supernatants were incubated with an anti-GFP antibody and nProtein A-Sepharose 4 Fast Flow for 2 h at 4 °C. The beads were washed with wash buffer (50 mM Tris-HCl, pH 7.5, 1% Triton X-100, 10% glycerol, 300 mM NaCl, 50 mM NaF, 1 mM Na_3VO_4, 10 μg/ml leupeptin, and 1 mM DTT) three times and boiled in sample buffer (62.5 mM Tris-HCl, pH 6.8, 5% 2-mercaptoethanol, 2% SDS, 5% sucrose, and 0.005% bromphenol

blue). Samples were subjected to SDS-PAGE and analyzed by immunoblotting using an anti-FLAG antibody.

Immunoblotting—Denatured proteins were resolved by SDS-PAGE and transferred to Immobilon-P membranes (Millipore, Billerica, MA). The membranes were blocked with skim milk and incubated with the appropriate antibodies. A horseradish peroxidase-conjugated anti-rabbit or mouse IgG antibody was used as the secondary antibody.

Subcellular Fractionation—RPE1 cells or HeLa cells expressing YFP-NDR2 were homogenized in homogenization buffer (20 mM HEPES-KOH, pH 7.4, 0.25 M sucrose, 1 mM dithiothreitol, and protease inhibitor mixture (Roche Diagnostics)) and centrifuged at 800 × *g* for 10 min at 4 °C to yield PNS fraction. Total organellar fraction and cytosolic fraction were prepared by centrifugation of the PNS fraction at 100,000 × *g* for 30 min. For fractionation by ultracentrifugation on an iodixanol density gradient, the PNS fraction of HeLa cells was mixed with iodixanol (Alere Technologies AS, Oslo, Norway) to yield a final 30% iodixanol solution. The PNS solution was loaded beneath a 14–26% iodixanol gradient and separated by ultracentrifugation in an SW41Ti rotor (Beckman Coulter) at 100,000 × *g* for 90 min at 4 °C. The gradient was collected into 12 fractions. Organelles in each fraction were pelleted by dilution with an equal volume of buffer and centrifugation at 100,000 × *g* for 20 min at 4 °C and subjected to immunoblot analysis.

Proteinase K Sensitivity Assay—The PNS fractions (140 μg of protein each) of YFP-NDR2-expressing RPE1 cells were treated with 1 μg/ml proteinase K for 2 min at 0 °C in the presence or absence of 1% Triton X-100. After terminating the reaction with 3 mg/ml phenylmethylsulfonyl fluoride, the PNS fraction was centrifuged at 100,000 × *g* for 30 min, and the resulting pellets were analyzed by SDS-PAGE and immunoblotting.

Reverse Transcription (RT)-PCR—RT-PCR was performed as described previously (47). Total RNA was isolated using an Isogen II kit (Nippon Gene, Tokyo, Japan) and reverse-transcribed to yield single-stranded cDNAs using a Transcriptor high fidelity cDNA synthesis kit (Roche Diagnostics). The cDNA fragments were amplified by PCR amplification using GoTaq DNA polymerase (Promega) and analyzed by agarose gel electrophoresis.

Assay for Primary Cilium Formation—An assay for primary cilium formation was carried out as described previously (12, 32). RPE1 cells were plated on coverslips in 35-mm plates at 1.0×10^5 cells/plate, transfected with 10 nM siRNAs using Lipofectamine RNAiMax (Invitrogen), cultured for 24 h, and then serum-starved for 48 h. In knockdown/rescue experiments, before siRNA transfection, cells were transfected with expression plasmids using FuGENE-HD and cultured for 4 h. Cells were fixed with 10% trichloroacetate and immunostained with anti-Ac-tubulin and anti-pericentrin antibodies. Alexa Fluor 568-labeled anti-mouse IgG and Alexa Fluor 633-labeled anti-rabbit IgG antibodies were used as secondary antibodies.

Statistical Analysis—Statistical data are represented as the means ± S.E. of three independent experiments. All statistical analyses were carried out using Prism 6 (GraphPad Software, La Jolla, CA). The *p* values were calculated using one-way ANOVA followed by Dunnett's test for multiple data set comparisons. In all cases, $p < 0.05$ was considered statistically significant.

Author Contributions—S. A. designed, performed, and analyzed the experiments shown in Figs. 1, 2, 4, 5, 7, and 9. T. N. and M. M. designed and performed the experiments shown in Figs. 3, 6, and 8. K. O. performed the experiments shown in Fig. 3. Y. H. performed the experiments shown in Fig. 2 and supplemental Movie S1. Y. F. produced several materials and provided intellectual input. K. M. conceived and designed the project and wrote the manuscript. All authors reviewed the results and approved the final version of the manuscript.

Acknowledgments—We thank Dr. Hiroyuki Nakanishi for providing the hTERT-RPE1 cells and Drs. Kazumasa Ohashi, Shuhei Chiba, Yuta Amagai, and Shigehiko Tamura for helpful discussions.

References

1. Hergovich, A., Stegert, M. R., Schmitz, D., and Hemmings, B. A. (2006) NDR kinases regulate essential cell processes from yeast to humans. *Nat. Rev. Mol. Cell Biol.* **7,** 253–264
2. Hergovich, A. (2013) Regulation and functions of mammalian LATS/NDR kinases: looking beyond canonical Hippo signalling. *Cell Biosci.* **3,** 32
3. Emoto, K. (2011) The growing role of the Hippo-NDR kinase signaling in neuronal development and disease. *J. Biochem.* **150,** 133–141
4. Nagai, T., and Mizuno, K. (2014) Multifaceted roles of Furry proteins in invertebrates and vertebrates. *J. Biochem.* **155,** 137–146
5. Cornils, H., Kohler, R. S., Hergovich, A., and Hemmings, B. A. (2011) Human NDR kinases control G_1/S cell cycle transition by directly regulating p21 stability. *Mol. Cell Biol.* **31,** 1382–1395
6. Vichalkovski, A., Gresko, E., Cornils, H., Hergovich, A., Schmitz, D., and Hemmings, B. A. (2008) NDR kinase is activated by RASSF1A/MST1 in response to Fas receptor stimulation and promotes apoptosis. *Curr. Biol.* **18,** 1889–1895
7. Hergovich, A., Lamla, S., Nigg, E. A., and Hemmings, B. A. (2007) Centrosome-associated NDR kinase regulates centrosome duplication. *Mol. Cell* **25,** 625–634
8. Chiba, S., Ikeda, M., Katsunuma, K., Ohashi, K., and Mizuno, K. (2009) MST2- and Furry-mediated activation of NDR1 kinase is critical for precise alignment of mitotic chromosomes. *Curr. Biol.* **19,** 675–681
9. Ultanir, S. K., Hertz, N. T., Li, G., Ge, W. P., Burlingame, A. L., Pleasure, S. J., Shokat, K. M., Jan, L. Y., and Jan, Y. N. (2012) Chemical genetic identification of NDR1/2 kinase substrates AAK1 and Rabin8 uncovers their roles in dendrite arborization and spine development. *Neuron* **73,** 1127–1142
10. Cornils, H., Stegert, M. R., Hergovich, A., Hynx, D., Schmitz, D., Dirnhofer, S., and Hemmings, B. A. (2010) Ablation of the kinase NDR1 predisposes mice to the development of T cell lymphoma. *Sci. Signal.* **3,** ra47
11. Zhang, L., Tang, F., Terracciano, L., Hynx, D., Kohler, R., Bichet, S., Hess, D., Cron, P., Hemmings, B. A., Hergovich, A., and Schmitz-Rohmer, D. (2015) NDR functions as a physiological YAP1 kinase in the intestinal epithelium. *Curr. Biol.* **25,** 296–305
12. Chiba, S., Amagai, Y., Homma, Y., Fukuda, M., and Mizuno, K. (2013) NDR2-mediated Rabin8 phosphorylation is crucial for ciliogenesis by switching binding specificity from phosphatidylserine to Sec15. *EMBO J.* **32,** 874–885
13. Fliegauf, M., Benzing, T., and Omran, H. (2007) When cilia go bad: cilia defects and ciliopathies. *Nat. Rev. Mol. Cell Biol.* **8,** 880–893
14. Goetz, S. C., and Anderson, K. V. (2010) The primary cilium: a signalling centre during vertebrate development. *Nat. Rev. Genet.* **11,** 331–344
15. Sung, C. H., and Leroux, M. R. (2013) The roles of evolutionarily conserved functional modules in cilia-related trafficking. *Nat. Cell Biol.* **15,** 1387–1397
16. Knödler, A., Feng, S., Zhang, J., Zhang, X., Das, A., Peränen, J., and Guo, W. (2010) Coordination of Rab8 and Rab11 in primary ciliogenesis. *Proc. Natl. Acad. Sci. U.S.A.* **107,** 6346–6351
17. Westlake, C. J., Baye, L. M., Nachury, M. V., Wright, K. J., Ervin, K. E., Phu, L., Chalouni, C., Beck, J. S., Kirkpatrick, D. S., Slusarski, D. C., Sheffield,

V. C., Scheller, R. H., and Jackson, P. K. (2011) Primary cilia membrane assembly is initiated by Rab11 and transport protein particle II (TRAPPII) complex-dependent trafficking of Rabin8 to the centrosome. *Proc. Natl. Acad. Sci. U.S.A.* **108,** 2759–2764

18. Goldstein, O., Kukekova, A. V., Aguirre, G. D., and Acland, G. M. (2010) Exonic SINE insertion in STK38L causes canine early retinal degeneration (erd). *Genomics* **96,** 362–368
19. Berta, Á. I., Boesze-Battaglia, K., Genini, S., Goldstein, O., O'Brien, P. J., Szél, Á., Acland, G. M., Beltran, W. A., and Aguirre, G. D. (2011) Photoreceptor cell death, proliferation and formation of hybrid rod/S-cone photoreceptors in the degenerating STK38L mutant retina. *PLoS One* **6,** e24074
20. Devroe, E., Erdjument-Bromage, H., Tempst, P., and Silver, P. A. (2004) Human Mob proteins regulate the NDR1 and NDR2 serine-threonine kinases. *J. Biol. Chem.* **279,** 24444–24451
21. Smith, J. J., and Aitchison, J. D. (2013) Peroxisomes take shape. *Nat. Rev. Mol. Cell Biol.* **14,** 803–817
22. Ma, C., Agrawal, G., and Subramani, S. (2011) Peroxisome assembly: matrix and membrane protein biogenesis. *J. Cell Biol.* **193,** 7–16
23. Fujiki, Y., Okumoto, K., Mukai, S., Honsho, M., and Tamura, S. (2014) Peroxisome biogenesis in mammalian cells. *Front. Physiol.* **5,** 307
24. Hettema, E. H., Erdmann, R., van der Klei, I., and Veenhuis, M. (2014) Evolving models for peroxisome biogenesis. *Curr. Opin. Cell Biol.* **29,** 25–30
25. Waterham, H. R., Ferdinandusse, S., and Wanders, R. J. (2016) Human disorders of peroxisome metabolism and biogenesis. *Biochim. Biophys. Acta* **1863,** 922–933
26. Gould, S. J., Keller, G. A., Hosken, N., Wilkinson, J., and Subramani, S. (1989) A conserved tripeptide sorts proteins to peroxisomes. *J. Cell Biol.* **108,** 1657–1664
27. Swinkels, B. W., Gould, S. J., and Subramani, S. (1992) Targeting efficiencies of various permutations of the consensus C-terminal tripeptide peroxisomal targeting signal. *FEBS Lett.* **305,** 133–136
28. Miura, S., Kasuya-Arai, I., Mori, H., Miyazawa, S., Osumi, T., Hashimoto, T., and Fujiki, Y. (1992) Carboxyl-terminal consensus Ser-Lys-Leu-related tripeptide of peroxisomal proteins functions *in vitro* as a minimal peroxisome-targeting signal. *J. Biol. Chem.* **267,** 14405–14411
29. Matsumura, T., Otera, H., and Fujiki, Y. (2000) Disruption of the interaction of the longer isoform of Pex5p, Pex5pL, with Pex7p abolishes peroxisome targeting signal type 2 protein import in mammals: study with a novel *PEX5*-impaired Chinese hamster ovary cell mutant. *J. Biol. Chem.* **275,** 21715–21721
30. Goetz, S. C., Liem, K. F., Jr., and Anderson, K. V. (2012) The spinocerebellar ataxia-associated gene *tau tubulin kinase* 2 controls the initiation of ciliogenesis. *Cell* **151,** 847–858
31. Čajánek, L., and Nigg, E. A. (2014) Cep164 triggers ciliogenesis by recruiting Tau tubulin kinase 2 to the mother centriole. *Proc. Natl. Acad. Sci. U.S.A.* **111,** E2841–E2850
32. Oda, T., Chiba, S., Nagai, T., and Mizuno, K. (2014) Binding to Cep164, but not EB1, is essential for centriolar localization of TTBK2 and its function in ciliogenesis. *Genes Cells* **19,** 927–940
33. Elgersma, Y., Vos, A., van den Berg, M., van Roermund, C. W. T., van der Sluijs, P., Distel, B., and Tabak, H. F. (1996) Analysis of the carboxyl-terminal peroxisomal targeting signal 1 in a homologous context in *Saccharomyces cerevisiae*. *J. Biol. Chem.* **271,** 26375–26382
34. Mohan, K. V. K., Som, I., and Atreya, C. D. (2002) Identification of a type 1 peroxisomal targeting signal in a viral protein and demonstration of its targeting to the organelle. *J. Virol.* **76,** 2543–2547
35. Mast, F. D., Rachubinski, R. A., and Aitchison, J. D. (2015) Signaling dynamics and peroxisomes. *Curr. Opin. Cell Biol.* **35,** 131–136
36. Zhang, J., Kim, J., Alexander, A., Cai, S., Tripathi, D. N., Dere, R., Tee, A. R., Tait-Mulder, J., Di Nardo, A., Han, J. M., Kwiatkowski, E., Dunlop, E. A., Dodd, K. M., Folkerth, R. D., Faust, P. L., *et al.* (2013) A tuberous sclerosis complex signalling node at the peroxisome regulates mTORC1 and autophagy in response to ROS. *Nat. Cell Biol.* **15,** 1186–1196
37. Watters, D., Kedar, P., Spring, K., Bjorkman, J., Chen, P., Gatei, M., Birrell, G., Garrone, B., Srinivasa, P., Crane, D. I., and Lavin, M. F. (1999) Localization of a portion of extranuclear ATM to peroxisomes. *J. Biol. Chem.* **274,** 34277–34282
38. Zhang, J., Tripathi, D. N., Jing, J., Alexander, A., Kim, J., Powell, R. T., Dere, R., Tait-Mulder, J., Lee, J. H., Paull, T. T., Pandita, R. K., Charaka, V. K., Pandita, T. K., Kastan, M. B., and Walker, C. L. (2015) ATM functions at the peroxisome to induce pexophagy in response to ROS. *Nat. Cell Biol.* **17,** 1259–1269
39. Dixit, E., Boulant, S., Zhang, Y., Lee, A. S., Odendall, C., Shum, B., Hacohen, N., Chen, Z. J., Whelan, S. P., Fransen, M., Nibert, M. L., Superti-Furga, G., and Kagan, J. C. (2010) Peroxisomes are signaling platforms for antiviral innate immunity. *Cell* **141,** 668–681
40. Lazarow, P. B. (2011) Viruses exploiting peroxisomes. *Curr. Opin. Microbiol.* **14,** 458–469
41. Harano, T., Nose, S., Uezu, R., Shimizu, N., and Fujiki, Y. (2001) Hsp70 regulates the interaction of the peroxisome targeting signal type 1 (PTS1)-receptor Pex5p and PTS1. *Biochem. J.* **357,** 157–165
42. Gouveia, A. M. M., Reguenga, C., Oliveira, M. E. M., Sa-Miranda, C., and Azevedo, J. E. (2000) Characterization of peroxisomal Pex5p from rat liver. Pex5p in the Pex5p-Pex14p membrane complex is a transmembrane protein. *J. Biol. Chem.* **275,** 32444–32451
43. Zaki, M. S., Heller, R., Thoenes, M., Nürnberg, G., Stern-Schneider, G., Nürnberg, P., Karnati, S., Swan, D., Fateen, E., Nagel-Wolfrum, K., Mostafa, M. I., Thiele, H., Wolfrum, U., Baumgart-Vogt, E., and Bolz, H. J. (2016) PEX6 is expressed in photoreceptor cilia and mutated in deafblindness with enamel dysplasia and microcephaly. *Hum. Mutat.* **37,** 170–174
44. Martin, C. A., Ahmad, I., Klingseisen, A., Hussain, M. S., Bicknell, L. S., Leitch, A., Nürnberg, G., Toliat, M. R., Murray, J. E., Hunt, D., Khan, F., Ali, Z., Tinschert, S., Ding, J., Keith, C., *et al.* (2014) Mutations in PLK4, encoding a master regulator of centriole biogenesis, cause microcephaly, growth failure and retinopathy. *Nat. Genet.* **46,** 1283–1292
45. Shimizu, N., Itoh, R., Hirono, Y., Otera, H., Ghaedi, K., Tateishi, K., Tamura, S., Okumoto, K., Harano, T., Mukai, S., and Fujiki, Y. (1999) The peroxin Pex14p: cDNA cloning by functional complementation on a Chinese hamster ovary cell mutant, characterization, and functional analysis. *J. Biol. Chem.* **274,** 12593–12604
46. Otera, H., Okumoto, K., Tateishi, K., Ikoma, Y., Matsuda, E., Nishimura, M., Tsukamoto, T., Osumi, T., Ohashi, K., Higuchi, O., and Fujiki, Y. (1998) Peroxisome targeting signal type 1 (PTS1) receptor is involved in import of both PTS1 and PTS2: studies with PEX5-defective CHO cell mutants. *Mol. Cell Biol.* **18,** 388–399
47. Abiko, H., Fujiwara, S., Ohashi, K., Hiatari, R., Mashiko, T., Sakamoto, N., Sato, M., and Mizuno, K. (2015) Rho guanine nucleotide exchange factors involved in cyclic-stretch-induced reorientation of vascular endothelial cells. *Mol. Biol. Cell* **128,** 1683–1695